Rab4 and Rab11 coordinately regulate the recycling of angiotensin II type I receptor as demonstrated by fluorescence resonance energy transfer microscopy

Hewang Li
Hui-Fang Li
Georgetown University Medical Center
Department of Pediatrics
Washington, DC 20057

Robin A. Felder
University of Virginia Health Sciences Center
Department of Pathology
Charlottesville, Virginia 22908

Ammasi Periasamy
University of Virginia
Department of Biology and Biomedical Engineering
Keck Center for Cellular Imaging (KCCI)
Charlottesville, Virginia 22904

Pedro A. Jose
Georgetown University Medical Center
Department of Pediatrics
Washington, DC 20057

Abstract. The recycling of G-protein-coupled receptors (GPCR) to the cell surface after internalization plays an important role in the regulation of overall GPCR activity. The angiotensin II type I receptor (AT_1R) belongs to class B GPCRs that recycle slowly back to the cell surface. Previous studies have proposed that Rab11 controls the recycling of AT_1R; however, recent reports show that Rab4, a rapid recycling regulator, co-localizes also with internalized AT_1R. Different from the subcellular co-localization provided by fluorescence microscopy, fluorescence resonance energy transfer (FRET) microscopy provided the spatial relationship of AT_1R with Rab4 and Rab11 in the nanometer-range proximity during the entire course of AT_1R recycling. During the early recycling stage, internalized AT_1Rs were mainly associated with Rab4 in the cytoplasm. During the mid-recycling stage, AT_1Rs were associated with both Rab4 and Rab11 in the perinuclear compartments. However, during the late-recycling stage, AT_1Rs were mainly associated with Rab11, both in the perinuclear compartments and the plasma membrane. Co-immunoprecipitation data confirmed these dynamic associations, which were disrupted by silencing of either the Rab4 or Rab11 gene. Based on these observations, we propose a Rab4 and Rab11 coordinated model for AT_1R recycling. © *2008 Society of Photo-Optical Instrumentation Engineers.* [DOI: 10.1117/1.2943286]

1 Introduction

The binding of angiotensin II (Ang II) to the Ang II type I receptor (AT_1R), a member of the superfamily of G-protein-coupled receptors (GPCRs), activates $G_{q/11}$ and initiates a series of intracellular processing,[1–3] including rapid phosphorylation, desensitization, and endocytosis of the AT_1R. The internalized AT_1R, via clathrin-coated vesicles (CCV), binds to β-arrestins and dynamin.[4,5] CCVs fuse with sorting endosomes shortly after internalization with participation of a number of Rab GTPases.

The Rab family proteins are a 23-25kDa ras superfamily of GTPases that contain two C-terminal geranylgeranyl (20 carbons) groups serving to bind proteins tightly to membranes.[6] To date, over 60 mammalian Rab proteins have been identified; each Rab protein appears to associate with a particular membrane compartment(s) and regulate intracellular protein trafficking, such as endocytosis, endosome fusion, exocytosis, and recycling of GPCRs.[7,8]

It is believed that two distinct intracellular systems regulate the recycling of internalized GPCRs: one is the Rab4-mediated rapid recycling pathway, and the other is the Rab11-mediated slow endosome pathway.[5–9] Rab4 is mainly localized in early endosomes and is thought to play an important role in the efflux of cargo proteins out of early endosomes and the rapid recycling of cargo proteins directly to the plasma membrane from the early endosome.[10,11] Rab11 is mainly localized in perinuclear recycling endosomes and the trans-Golgi network and regulates the slow recycling from perinuclear endosomes and the trans-Golgi network to the plasma membrane.[12,13]

Internalized GPCRs recycle back to the cell surface through different pathways.[5,8] Based on their affinity to and association with β-arrestins, GPCRs are divided into two classes[4]: class A receptors, which bind weakly with β-arrestins and recycle rapidly back to the plasma membrane, and class B receptors, which bind tightly with β-arrestins and recycle slowly back to the plasma membrane. The rapid recycling of β_2-adrenogenic receptor (β_2AR), a typical class A GPCR, appears to be regulated by Rab4, directly from early endosomes,[14] and may[15] or may not[16] be regulated by Rab11. AT_1R, a typical class B GPCR, is suggested to be regulated by Rab11 for its recycling.[16,17] Overexpression of wild-type Rab11 and constitutively active Rab11 (Q70L) significantly

Address all correspondence to Pedro A. Jose, MD, PhD, Professor of Pediatrics and Physiology and Biophysics, Georgetown University Medical Center, Washington, DC 20007; Tel: 202–444–8675; Fax: 202–444–7161; E-mail: pjose01@georgetown.edu

increases $AT_{1A}R$ recycling to the plasma membrane.[16] Several studies have indicated that Rab11 also regulates the recycling of other class B GPCRs, such as vasopressin V2 receptor,[18] CXC chemokine receptor 2,[19] β-isoform of the thromboxane A2 receptor,[20] and M4 muscarinic acetylcholine receptor.[21] Recently, Rab4 has also been suggested to participate in AT_1R recycling.[22] Thus, the roles of Rab4, Rab11, or both in the recycling of the AT_1R are not well understood.

In the current study, fluorescence resonance energy transfer (FRET) microcopy[23] was employed to detect the dynamic relationship between AT_1R and endogenous Rab4 or Rab11 during the 3 h of the entire recycling course after the internalization of AT_1R. FRET is a powerful tool to detect protein-protein interaction of less than 10-nm distance,[24] and it can overcome the limitation (resolution is hundreds of nm) of the methods used in most of previous studies on the morphological co-localization of Rab4 and Rab11 with the cargo GPCR. Moreover, some of the Rab-dominant negative mutants used in several studies are not GTPase-defective, as originally presumed.[25] Here, we provide additional insights into the relationship between Rab4/Rab11 and AT_1R recycling. We observed that both Rab4 and Rab11 are associated with the AT_1R recycling, and the association varies depending upon the recycling stage, as observed by FRET microscopy and co-immunoprecipitation. Moreover, gene knockdown of either Rab4 or Rab11 by specific siRNAs disrupts their dynamic association and AT_1R recycling. Based on these studies, we propose a model of a Rab4 and Rab11 coordinated regulation of AT_1R recycling.

2 Materials and Methods

2.1 Antibodies and Reagents

Monoclonal mouse Rab4 and Rab11 antibodies were purchased from BD Transduction Laboratories (Lexington, Kentucky). Polyclonal rabbit anti-GFP, polyclonal rabbit anti-Rab4, and polyclonal goat anti-Rab11 and normal mouse, rabbit, and goat antibodies were obtained from Santa Cruz Biotechnology (Santa Cruz, California). Alexa-546, Alexa-555, and Alexa-633 protein labeling kits were obtained from Molecular Probes (Eugene, Oregon). Cycloheximide and other obtained reagents were obtained from Sigma (St. Louis, MO).

2.2 Cell Culture and Transfection

Human embryonic kidney (HEK) 293 cells from ATCC (Manassas, Virginia) were cultured in Dulbecco's modified Eagle's medium (DMEM) (Invitrogen) containing 4.5 g/L glucose, 10% fetal bovine serum (FBS), 2 mM L-glutamine, and 1 mM sodium pyruvate. Human AT_1R-EGFP (enhanced green fluorescence protein) or its empty vector pEGFP-N1[26] was transfected into HEK 293 cells using Lipofectamine 2000 transfection reagents (Invitrogen), as described previously,[27] according to the manufacturer's instructions. Transfectants were selected with G418. Stable transfectants were tested and confirmed by immunoblotting with anti-GFP and anti-AT_1R antibodies, flow cytometry, and radioligand binding assay (data not shown). The EGFP tag did not interrupt the function of AT_1R, determined by a dose-dependent Ang II–induced phosphorylation of extracellular signal-regulated kinase

(ERK1/2) (data not shown). The stably transfected cells expressing human AT_1R-EGFP were designated in this study as AT_1R HEK 293 cells.

2.3 siRNA and Transfection

Specific Rab4 (AATGCAGGAACTGGCAAATCT), Rab11 (AAGAGTAATCTCCTGTCTCGA), and negative control (AATTCTCCGAACGTGTCACGT) siRNA duplexes were purchased from Qiagen (Valencia, California). AT_1R HEK 293 cells were transfected with these siRNA using Lipofectamine 2000 transfection reagents (Invitrogen) according to the manufacturer's instructions. After siRNA treatment for 36 h, cells were split into three portions. A small portion of cells was used to check Rab4 and Rab11 levels by immunoblotting with anti-Rab4 and Rab11 antibodies [Fig. 1(b)]. The largest portion of cells was used for immunoprecipitation experiments [Fig. 1(c)]. The third portion of the cells was dispersed in DMEM containing 10% FBS and placed (5×10^4 cells per well) on six-well plates with collagen I-coated coverslips; the attached cells were gently washed and fixed with 4% formaldehyde in PBS for observation of AT_1R-EGFP fluorescence at the indicated recycling times after the cells have been treated with Ang II for 15 min (Fig. 2).

2.4 Immunoprecipitation and Immunoblotting

Vehicle- or siRNA-transfected AT_1R HEK 293 cells were homogenized by freeze-thaw ($5 \times$) in a lysis buffer (20 mM Tris·HCl, pH 8.0/1 mM EDTA/1 mM NaN_3/2 mM DTT/0.25 M sucrose), with 0.5 mM 4-(2-aminoethyl)benzenesulfonyl fluoride (AEBSF), 0.5 mM benzamidine hydrochloride, and protease inhibitors (soybean and lima bean trypsin inhibitors, leupeptin, and aprotinin, each 1 μg/ml). The homogenates (1 mg) were incubated (rocking, 4°C, 4 h) with 5 μg of anti-GFP rabbit IgG, 4 μg of anti-Rab4 rabbit IgG, or 6 μg of anti-Rab11 goat IgG in 0.5 ml of the lysis buffer with 20 μM $MgCl_2$, 0.1% ovalbumin, 0.5 mM AEBSF, 0.5% 3-[(3-cholamidopropyl)dimethylammonio]-1-propanesulfonate. Controls were normal rabbit, mouse, or goat IgG (data not shown). After adding 60 μl of a 50% slurry of protein G-Sepharose CL-4B (Amersham Pharmacia, Uppsala, Sweden) in PBS and incubation at 4°C overnight, the beads were washed three times with 1 ml of ice-cold PBS, containing 0.5 mM AEBSF. Proteins bound to beads were eluted in 80 μl of loading buffer at 65°C for 10 min, separated by SDS/PAGE (sodium dodecyl sulfate/polyacrylamide gel electrophoresis) in 4 to 12% gradient gels, and transferred onto nitrocellulose membrane for incubation with mAb against Rab4 or Rab11 and rabbit anti-GFP, followed by appropriate horseradish peroxidase-conjugated secondary antibodies and detection using Super Signal Chemiluminescent substrate (Pierce, Rockford, IL).

2.5 Confocal Immunofluorescence Microscopy

AT_1R HEK 293 cells were fixed with 4% paraformaldehyde in PBS for 20 min at room temperature. After washing with PBS, the fixed cells on coverslips were incubated overnight at 4°C with Alexa Fluor 633-conjugated monoclonal mouse Rab4 antibody (2 μg/ml; Alexa Fluor 633 protein labeling kit, Molecular Probe, Eugene, Oregon) or Alexa Fluor 546-conjugated polyclonal goat Rab11 antibody (5 μg/ml; Alexa
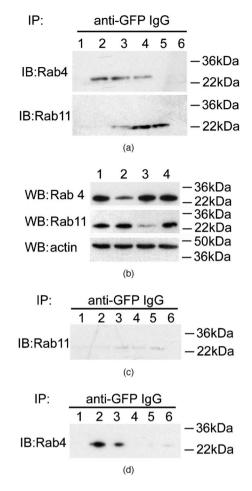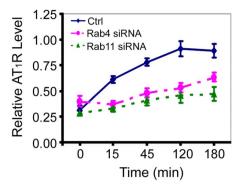
Fig. 1 Co-immunoprecipitation of AT_1R, Rab4, and Rab11. (a) AT_1R HEK 293 cells treated without (lane 1) or with Ang II (100 nM, 15 min) were co-immunoprecipitated following the procedure described in Sec. 2 for recovery of 0 (lane 2), 15 (lane 3), 45 (lane 4), 120 (lane 5), and 180 (lane 6) min, respectively. Cell homogenates were incubated with anti-GFP IgG (5 μg), and precipitated proteins were separated by SDS-PAGE and immunoblotted with Rab4 or Rab11 mAbs, as indicated. (b) 30 μg protein homogenates from AT_1 HEK 293 cells untreated (lane 1) or treated with Rab4 (lane 2) or Rab11 (lane 3) siRNA and negative control siRNAs (lane 4) were immunoblotted with antibodies against Rab4, Rab11, or actin, as indicated. (c) As in (a), Rab4 siRNA-transfected cells were treated without (lane 1) or with Ang II (100 nM, 15 min) following recovery of 0 (lane 2), 15 (lane 3), 45 (lane 4), 120 (lane 5), and 180 (lane 6) min, respectively. Cell homogenates were precipitated with anti-GFP IgG (5 μg) and immunoblotted with Rab11 mAb. (d) As in (c), Rab11 siRNA-trasnfected cells were treated without (lane 1) or with Ang II (100 nM, 15 min) following recovery of 0 (lane 2), 15 (lane 3), 45 (lane 4), 120 (lane 5), and 180 (lane 6) min, respectively. Cell homogenates were precipitated with anti-GFP IgG (5 μg) and immunoblotted with Rab4 mAb.

Fluor 546 protein labeling kit, Molecular Probe). The coverslips were mounted in SlowFade mounting medium (Molecular Probe) and sealed onto glass slides. Samples were imaged using an Olympus Fluoview FV300 laser scanning confocal microscope equipped with a 60× / 1.4 NA objective.

2.6 Receptor Recycling Assays

Vehicle- or siRNA-transfected AT_1R HEK 293 cells were treated with vehicle or 100 nM Ang II for 15 min at 37°C

Fig. 2 Interruption of AT_1R recycling with either Rab4 or Rab11 gene silencing. AT_1R HEK 293 cells were transfected without (solid line) or with either Rab4 siRNA (broken line) or Rab11 siRNA (dashed line) for 36 h. Then, cells were treated as described in Sec. 2. The amount of cell surface AT_1R was assessed by the average intensity of AT_1R fluorescence at the plasma membrane using Metamorph 7.0. Data are mean±SE, $n=4-6$.

and then placed on ice. After washing three times with ice-cold, serum-free DMEM medium, the cells were recultured in complete culture medium containing 20 μg/ml cycloheximide and reincubated at 37°C (with 5% CO_2) for the indicated time from 0 to 180 min. The cells were then fixed with 4% paraformaldehyde for fluorescence microscopy. The density of AT_1R at the cell surface was determined by quantifying cell surface fluorescence using MetaMorph 7.0 (Molecular Devices, Downington, Pennsylvania).[27] After identifying the plasma membrane, regions of interest (ROIs) were drawn manually in 300× zoomed-in images. The background was subtracted from each image, and then the images were thresholded to identify specific EGFP fluorescence for AT_1R at the plasma membrane. Receptor recycling was defined as the recovery of cell-surface receptors following the removal of Ang II, compared with the cell-surface expression of receptors in cells that were not exposed to Ang II (vehicle-treated cells).

2.7 FRET Microscopy and Data Processing

The fluorophore pairs used for FRET imaging in this study were AT_1R-EGFP (as donor dipole) and Alexa Fluor 555 (as acceptor dipole) conjugated with Rab4 or Rab11 antibodies (Alexa Fluor 555 protein labeling kit, Molecular Probe). Seven images were acquired for each FRET analysis, as described,[23] with an Olympus Fluoview FV300 laser scanning confocal microscope equipped with a 60× / 1.4 NA objective, Argon (488 nm) and HeNe (543 nm) laser, and emission filters 515/50 nm and 590-nm long press (LP) filter. Either single-labeled donor or acceptor or double-labeled samples were acquired under the same conditions throughout the image collection. The uncorrected FRET images (uFRET) were acquired by donor excitation in the acceptor channel, which contained pure FRET (pFRET) and contaminations from both donor and acceptor spectral bleed-through (SBT). pFRET images were generated by employing a described algorithm[23] for pixel-by-pixel removal of donor and acceptor SBT on the basis of matched fluorescence levels between the double-labeled specimen and the single-labeled reference specimens.

ROIs were selected in the uFRET images.[23] In this study, we used image (e) (donor excitation in the donor channel of

the double-labeled specimen) as the reference image for selection of ROIs to determine the plasma membrane, cytoplasm, and perinuclear compartments. Image g was acquired at acceptor excitation in the acceptor channel of the double-labeled specimen.

The percentage of energy transfer efficiency ($E\%$) images was processed on a pixel-by-pixel basis by using the following equation:

$$E\% = 1 - \{Ida/(Ida + pFRET \times (Pd/Pa) \times (Sd/Sa)$$
$$\times (Qd/Qa) \},$$

where Pd and Pa are the photo multiplier tube (PMT) gains of donor and acceptor channels; Sd and Sa are the spectral sensitivity of donor and acceptor channels provided by the manufacturer; Qd and Qa are the donor and acceptor quantum yield, measured by spectrofluorometer, as described[28]; Ida is the image of donor excitation in the donor channel of the double-label samples after removing the background; and $pFRET$ is the "processed FRET" or "pure FRET." The calculation of distance of donor and acceptor (r) was based on the equation as described in Ref. 23: $r = R_0[(1/E)-1]^{1/6}$; Förster's distance R_0 in this study was 67.5 Å.

2.8 Statistical Analysis

Results are expressed as mean (M) $\pm$ standard error (SE), as indicated. Significant differences among groups were determined by factorial ANOVA and the Student-Newman-Keuls test. $P < 0.05$ was considered statistically significant (SigmaStat 3.0, SPSS, Inc., Chicago).

3 Results

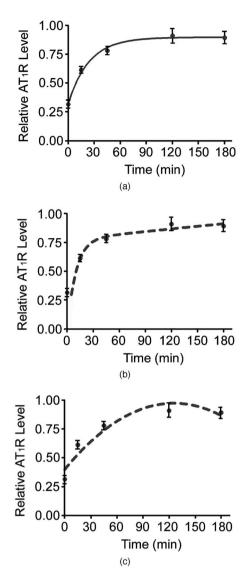### 3.1 Subcellular Location of Human AT$_1$R, Rab4, and Rab11

In HEK 293 cells under basal conditions, human AT$_1$R tagged with EGFP was observed primarily at the plasma membrane [Fig. 3(a)] but also in the intracellular membrane, perinuclear compartments, and cytoplasm [Fig. 3(a)], consistent with previous observations.[22,27]

Endogenous Rab4 staining was observed in typical vesicles scattered throughout the cytoplasm, and very occasionally concentrated in the perinuclear compartments [Fig. 3(b)]. Endogenous Rab11 was scattered throughout the cytoplasm as well, but most often, Rab11 was observed to concentrate in the perinuclear areas [Fig. 3(c)]. Overall, Rab4 was more dispersed than Rab11 throughout the cytoplasm, but neither Rab4 nor Rab11 was observed at the plasma membrane. These observations are in agreement with studies using GFP-tagged Rab4 and Rab11.[6,22]

Minimal, if any, co-localization was observed between AT$_1$R and Rab4 [Fig. 3(d)] or Rab11 [Fig. 3(e)]. Few co-localizations were observed among AT$_1$R, Rab4, and Rab11 [Fig. 3(f)].
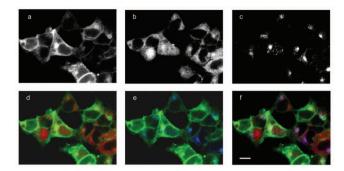
3.2 Recycling Course of AT$_1$R

In this report, the cell surface AT$_1$R at the basal state was set at 100%. As shown in Fig. 4, the relative surface intensity of AT$_1$R is $31.8 \pm 5.3\%$ ($n=33$ cells) when cells were treated with 100 nM Ang II for 15 min, a time considered as the start

Fig. 4 Recycling of AT$_1$R to the cell surface. AT$_1$R HEK 293 cells were stimulated with Ang II (100 nM, 15 min) and then were placed on ice. After thorough washing, the cells were incubated in complete culture medium containing 20 μg of cycloheximide at 37°C in 5% CO_2 for the indicated times. Then, cells were fixed with 4% paraformaldehyde, as described in Sec. 2. The amount of cell surface AT$_1$R was assessed by the average intensity of AT$_1$R fluorescence at the plasma membrane using Metamorph 7.0. Data are mean±SE; the data were plotted with first-order exponential fit (a), second-order exponential fit (b), and second-order polynomial fit (c), respectively, using OriginLab 6.1.
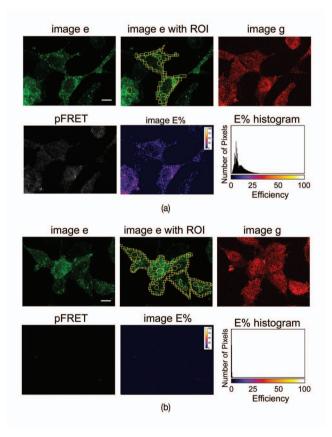
of recycling (time 0 min); subsequent recycling of AT$_1$R to the plasma membrane was quantified at the indicated time points after removing of Ang II. The membrane surface AT$_1$R fluorescence intensity was directly related to recovery time (t): $0.895 - 0.58e^{-t/23.8}$, which followed a first-order exponential curve [Fig. 4(a)]. After ~45 min, the cell surface AT$_1$R reached slightly over 75% of its basal level, and close to 90% of its basal level at about 2 h, similar to that reported[22] for the rat AT$_{1A}$R, but much slower than that[14,17] for class A GPCRs, e.g., β_2AR. However, only ~90% AT$_1$R was expressed at the plasma membrane at steady state (Fig. 4), probably due to

Fig. 3 Subcellular distribution of the AT_1R (a), Rab4 (b), and Rab11 (c) in AT_1R HEK 293 cells. The AT_1R, tagged with EGFP at its C-terminal, is mainly localized at the plasma membrane. Both Rab4 and Rab11 are scattered throughout the cytoplasm; portions of Rab11 reside in the perinuclear compartments. (d) Overlay of (a) (AT_1R-GFP, green) and (b) (Rab4, red); (e) overlay of (a) and (c) (Rab11, blue); (f) overlay of (a), (b), and (c). Bar, 10 μm.

the lack of newly synthesized AT_1R for replacement, implying that $\sim$10% of AT_1Rs were processed for degradation.

For a first-order exponential fit of the data, the following values are obtained: R^2 is 0.9931, with two degrees of free-
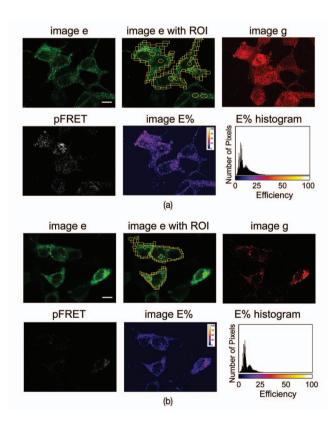
dom, and an absolute of square of 0.00168; the values for a second-order exponential fit [Fig. 4(b)] are: R^2 is 0.5833, with one degree of freedom, and an absolute of square is 0.1014. The second-order polynomial curve is a poor fit [Fig. 4(c)]. These analyses show that AT_1R recovery rate best fits a first-order exponential equation, consistent with a single recycling pathway for human AT_1R.

In the following studies, for convenience, we divided the entire recycling course into early (from time 0 to 15 min), middle (from 15 min to 45 min), and late (over 45 min) recycling stages.

3.3 Role of Rab4 and Rab11 in the Early Stage of AT_1R Recycling

FRET was not observed between AT_1R and Rab4 or Rab11 during the basal state (data not shown), which is consistent with the absence of co-localization of AT_1R with either Rab4 or Rab11 in the basal state (Fig. 3).

At the start of recycling (time 0), obvious FRET was observed in the cytoplasm between Rab4 and AT_1R [Fig. 5(a)], the efficiency of energy transfer (E%) was $28.3 \pm 9.1\%$ (n =34 cells), the estimated distance was 78.8 Å (Table 1), but no FRET was observed between Rab11 and AT_1R [Fig. 5(b), Table 1]. The association of AT_1R and Rab4, but not AT_1R

Fig. 5 FRET analysis of AT_1R and Rab4 (a) or AT_1R and Rab11 (b) at recycling time 0. As described in Sec. 2, regions of interest (ROIs) were drawn in image e, rectangles (□) indicate the plasma membrane, ovals (O) indicates cytoplasm, and freehand drawings indicate perinuclear compartments. The pFRET and $E\%$ images were processed by programs developed at the K. M. Keck Center for Cellular Imaging, University of Virginia (Charlottesville). Bar, 10 μm.

Fig. 6 FRET analysis of AT_1R and Rab4 (a) or AT_1R and Rab11 (b) at recycling time 15 min. As described in Sec. 2, ROIs were drawn in image e, rectangles (□) indicate the plasma membrane, ovals (O) indicate cytoplasm, and freehand drawings indicate perinuclear compartments. The pFRET and $E\%$ images were processed by programs developed at the K. M. Keck Center for Cellular Imaging, University of Virginia (Charlottesville). Bar, 10 μm.

Table 1 Calculation of efficiency of energy transfer (E%) and molecular proximity (R) between AT_1R and Rab4 or Rab11 during the entire AT_1R recycling course. AT_1R HEK 293 cells were treated and fixed as described in Sec. 2. AT_1R-EGFP is the donor; the acceptor is Rab4 or Rab11. FRET analysis is described in Figs. 5–9. Data are mean±SE; n, number of cells analyzed, Infin, infinity.

Recycling time (min)	Acceptor	n	Plasma membrane		Cytoplasm		Perinuclear compartment	
			E (%)	R(Å)	E (%)	R(Å)	E (%)	R(Å)
0	Rab4	34	0	infin	28.3±9.1	78.8	0	infin
	Rab11	34	0	infin	0	infin	0	infin
15	Rab4	35	0	infin	23.4±6.7	82.3	16.3±5.3	88.7
	Rab11	29	0	infin	11.6±3.3	94.7	14.9±7.8	90.2
45	Rab4	46	0	infin	21.0±2.1	84.2	34.5±4.1	75.1
	Rab11	36	0	infin	17.8±2.2	87.1	37.4±6.5	73.6
120	Rab4	25	0	infin	3.31±1.1	NA	0	infin
	Rab11	26	14.6±3.3	89.8	4.60±2.2	NA	13.8±2.1	91.6
180	Rab4	15	0	infin	0	infin	0	infin
	Rab11	15	0	infin	0	infin	0	infin

and Rab11 was also observed by immunoprecipitation [Fig. 1(a), lane 2].

At time 15 min, FRET was obvious between Rab4 and AT_1R in cytoplasm and perinuclear compartments, especially in vesicles in the cytoplasm [Fig. 6(a)], the E% was $23.4±6.7$% ($n=35$ cells) and $16.3±5.3$% ($n=35$ cells), respectively (Table 1). FRET was also observed between Rab11 and AT_1R [Fig. 6(b)] in perinuclear compartments ($14.9±7.8$%, $n=29$ cells) and cytoplasm ($11.6±3.3$, $n=29$ cells). No FRET was observed at the plasma membrane between AT_1R with either Rab4 or Rab11 (Fig. 6). The association of Rab4 and Rab11 with AT_1R was also observed by immunoprecipitation [Fig. 1(a), lane 3]. These observations indicated that Rab4 played a major role(s) during the early recycling period; Rab11 could also play some role in this stage.

3.4 Role of Rab4 and Rab11 in the Middle Stage of AT_1R Recycling

At time 45 min, FRET between Rab4 and AT_1R in the cytoplasm minimally decreased ($21.0±2.1$%, $n=46$ cells), but increased in perinuclear compartments ($34.5±4.1$%, $n=46$ cells) [Fig. 7(a); Table 1], compared to the early recycling stage. In contrast, FRET between Rab11 and AT_1R increased in both the cytoplasm ($17.84±2.2$%, $n=36$ cells) and perinuclear compartments ($37.4±6.5$%, $n=36$ cells) [Fig. 7(b)] compared to its early stage ($p<0.05$). At 45 min, no FRET was observed between AT_1R and Rab4 or Rab11 at the plasma membrane [Fig. 7; Table 1]. Of note, the calculated E% of Rab4 and AT_1R ($34.5±4.1$%, $n=46$ cells) was similar to that of Rab11 and AT_1R ($37.4±6.5$%, $n=36$ cells) ($p>0.05$); both Rab4 and Rab11 were co-

immunoprecipitated by the GFP antibody (for AT_1R) [Fig. 1(a), lane 4] and vice versa (data not shown). Furthermore, gene knockdown of Rab4 by specific Rab4 siRNA disrupted the association of AT_1R with Rab11 [Fig. 1(c)]; Rab11 gene knockdown also disrupted the association of Rab4 with AT_1R [Fig. 1(d)]. All of these data indicated that Rab4 and Rab11 were in the same recycling endosomes for AT_1R trafficking at this stage. Therefore, both Rab4 and Rab11 play important roles in AT_1R trafficking during this period.

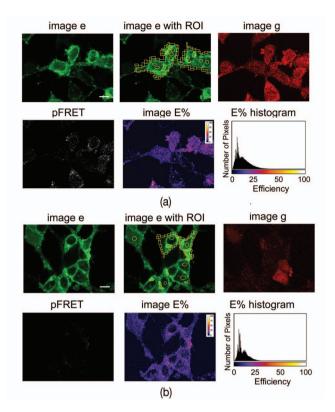### 3.5 Role of Rab4 and Rab11 in the Late Stage of AT_1R Recycling

At time 2 h, no FRET was observed between Rab4 and AT_1R in the cytoplasm, perinuclear compartments, and the plasma membrane [Fig. 8(a)], but obvious FRET was still observed between Rab11 and AT_1R in the perinuclear compartments [Fig. 8(b)]. The remarkable observation in this late period is that FRET occurred at the plasma membrane between Rab11 and AT_1R ($14.6±3.3$%, $n=26$ cells) [Fig. 8(b); Table 1], indicating the importance of Rab11 in the late stage of AT_1R recycling.

At time 3 h, no FRET was observed between Rab4 or Rab11 and AT_1R at the plasma membrane, cytoplasm, or perinuclear compartments (Fig. 9; Table 1), similar to that observed at the basal state (data not shown).

3.6 Interruption of AT_1R Recycling by Rab4, Rab11 Gene Silencing

The AT_1R recovery rate was markedly decreased in either Rab4 or Rab11 siRNA- treated cells (Fig. 2), which confirmed the conclusion obtained from the FRET studies that both Rab4 and Rab11 regulate the recycling of AT_1R.
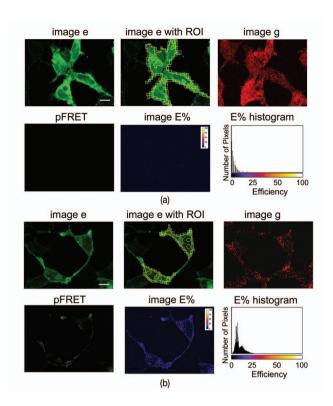
Fig. 7 FRET analysis of AT_1R and Rab4 (a) or AT_1R and Rab11 (b) at recycling time 45 min. As described in Sec. 2, ROIs were drawn in image e, rectangles (□) indicate the plasma membrane, ovals (O) indicate cytoplasm, and freehand drawings indicate perinuclear compartments. The pFRET and $E\%$ images were processed by programs developed at the K. M. Keck Center for Cellular Imaging, University of Virginia (Charlottesville). Bar, 10 μm.

Fig. 8 FRET analysis of AT_1R and Rab4 (a) or AT_1R and Rab11 (b) at recycling time 2 h. As described in Sec. 2, ROIs were drawn in image e, rectangles (□) indicate the plasma membrane, ovals (O) indicate cytoplasm, and freehand drawings indicate perinuclear compartments. The pFRET and $E\%$ images were processed by programs developed at the K. M. Keck Center for Cellular Imaging, University of Virginia (Charlottesville). Bar, 10 μm.

3.7 Relationship of Rab4 and Rab11 During the Entire AT_1R Recycling Course

In the basal state [Fig. 10(a)] and the start of recycling, time 0 [Fig. 10(b)] no co-localization was observed between Rab4 and Rab11. At 15 min [Fig. 10(c)] and 45 min [Fig. 10(d)], obvious co-localization of Rab4 and Rab11 was observed, and the greatest co-localization occurred at time 45 min, predominantly at perinuclear compartments. At the late stage of the recycling period, co-localization was no longer observed [Figs. 10(e) and 10(f)].
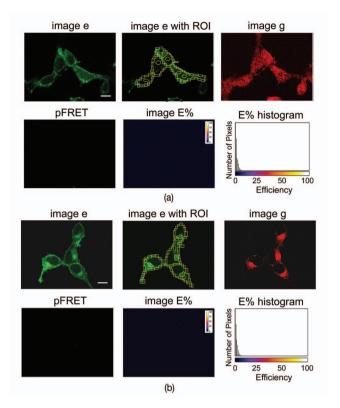
4 Discussion

The quantity of cell surface receptors is important for the cell to maintain its normal functions and responses to environmental changes.[1] Receptor expression on the cell surface is maintained by a dynamic balance among internalization, endocytosis, degradation, exocytosis, and recycling. The receptor recycling was initially thought to be a bulk flow process.[29] However, subsequent studies have shown that it is a regulated process. For example, the PDZ (PSD-95, Dlg, and ZO-1) motif[30] of β_2AR and the MRS (MOR-derived endocytic recycling sequence) sequence of μ opioid receptors[31] are important for their rapid recycling, respectively. In recent years, it has become widely appreciated that Rab4 and Rab11 are responsible for the regulation of receptor recycling.[5–11,32–36]

Transferrin receptor (Tfn) recycles efficiently to the cell surface via two distinct pathways: the rapid pathway is mediated by Rab4, while the slow pathway is initiated by tubular extension from sorting endosomes through Rab11-positive perinuclear endosomes.[5,35,36] It is also accepted that the Rab4-mediated rapid pathway is utilized for class A GPCR recycling, such as β_2AR, similar to the rapid pathway of Tfn. The class B GPCRs, including V2 vasopressin receptor,[18] m4AchR,[21] and somatostatin receptor,[37] recycle through the Rab11-mediated slow pathway, similar to the slow recycling of Tfn. AT_1R, which belongs to class B GPCR, recycles slowly back to the cell surface after internalization.[5,22]
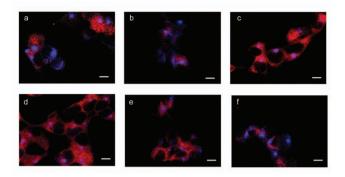
The molecular mechanism for AT_1R recycling has been controversial. ARAP1, or type 1 angiotensin II receptor-associated protein 1, has been shown to facilitate the AT_1R recycling to the cell surface,[38] but this mechanism is not yet fully accepted. Ferguson and co-workers[8,16] proposed a Rab11-mediated AT_1R slow recycling model after studying the role of wild-type Rab11 and constitutively active Rab11 (Q70L) in the recycling of the rat AT_1R. Hunyady et al.[22] have observed that Rab4 also co-localizes with AT_1R and proposed two distinct rat $AT_{1A}R$ recycling models, based on differential sensitivity to wortmannin, a PI3 kinase inhibitor. In the current study, both co-immunoprecipitation of AT_1R with Rab4 [Fig. 1(a)] and FRET was observed between Rab4 and AT_1R during the early (Figs. 5 and 6) and middle (Fig. 7) periods of AT_1R recycling, consistent with observations[22] that

Fig. 9 FRET analysis of AT$_1$R and Rab4 (a) or AT$_1$R and Rab11 (b) at recycling time 3 h. As described in Sec. 2, ROIs were drawn in image e, rectangles (□) indicate the plasma membrane, ovals (O) indicate cytoplasm, and freehand drawings indicate perinuclear compartments. The pFRET and $E\%$ images were processed by programs developed at the K. M. Keck Center for Cellular Imaging, University of Virginia (Charlottesville). Bar, 10 μm.

Fig. 10 Dynamic relationship between Rab4 and Rab11 during the AT$_1$R recycling course. At the basal state (a) and recycling time 0 (b), no co-localization exists between Rab4 and Rab11; at recycling time 15 min (c), a small portion of Rab11 is observed to co-localize with Rab4, and the calculated co-localization of Rab11 over Rab4 is 10.3±1.4%; at the middle stage of recycling, time 45 min (d), obvious co-localization between Rab4 and Rab11 is observed in the perinuclear compartments and the cytoplasm, and the calculated overall co-localization of Rab4 over Rab11 is 34.1±3.3%; at the late stage of recycling, times 2 h (e) and 3 h (f), no obvious co-localization is observed between Rab4 and Rab11. Red, Rab4; blue, Rab11; magenta, co-localization between Rab4 and Rab11. Data (mean ±SE) were from 24 to 65 cells per time point. Bar, 10 μm.

Rab4 also plays a role in the recycling of AT$_1$R. However, there may not be two separate Rab pathways for human AT$_1$R recycling: (1) during the entire AT$_1$R recycling period, no FRET between Rab4 and AT$_1$R was observed at the plasma membrane or subplasma membrane. Instead, FRET between AT$_1$R and Rab11 was observed at the plasma membrane or subplasma membrane at the late recycling stage [Fig. 8(b)]; (2) in the current study, the AT$_1$R recovery rate fits a first-order [Fig. 4(a)] but not second-order exponential equation [Figs. 4(b) and 4(c)], consistent with one sequential recycling pathway.

FRET is revolutionizing studies in life sciences and is widely applied in biology, biochemistry, immunology, cell and molecular biology, and clinical medicine to study protein-protein interaction, cellular signaling, conformational structure, ligand-receptor interaction, and diagnosis of certain diseases.[24] It is worthwhile to mention the advantage of pixel-by-pixel analysis in the current protocol, which enables the quantitative detection of FRET occurrence and removal of spectral bleedthrough from both donor and acceptor.[23] Pixel-by-pixel analysis also enables the detection of the spatial and temporal protein-protein interaction inside cells. Even though FRET can be measured at 10 to 100 Å distance of molecular proximity using the current protocol, the accurate location of a particular compartment is still challenging.
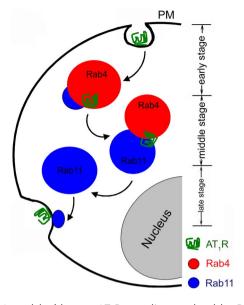
In the current study, FRET was observed and analyzed spatially into three compartments: the plasma membrane, cytoplasm, and perinuclear compartments. At the early stage of recycling, internalized human AT$_1$R were mainly in Rab4-positive compartments in the cytoplasm [Fig. 5(a)]. No FRET was observed between Rab4 and human AT$_1$R at the plasma membrane [Fig. 6(a)], indicating no rapid AT$_1$R recycling occurred with Rab4. At the middle stage, FRET of AT$_1$R with Rab4 and Rab11 was observed (Fig. 7), and the association of AT$_1$R with both Rab4 and Rab11 was supported by the co-IP data [Fig. 1(a)]. The association was disrupted by either Rab4 or Rab11 gene knockdown [Figs. 1(c) and 1(d)], indicating that AT$_1$R was localized mainly in compartments containing both Rab4 and Rab11 at this stage. However, at the late stage, AT$_1$R was localized mainly in Rab11-positive endosomes, both in the perinuclear compartments and at the plasma or subplasma membrane areas (Fig. 8). Rab4 or Rab11 gene knockdown decreased the AT$_1$R recovery rate (Fig. 2). Thus, our data indicate that both Rab4 and Rab11 coordinately regulate the entire recycling of AT$_1$R.

Based on the current and previous reports, a single recycling pathway for human AT$_1$R recycling coordinated by both Rab4 and Rab11 is proposed (Fig. 11). Internalized AT$_1$R rapidly appears in the CCVs. CCVs then fuse with Rab5/Rab4-positive early endosomes. The exact role(s) of Rab4 is not clear in the early endosomes, but it may enable the cargoed AT$_1$R vesicles to fuse with Rab11-positive perinuclear compartments. After the completion of fusion, Rab11 and Rab4 form common recycling endosomes mainly at the perinuclear compartments. Subsequently, the AT$_1$R destined for recycling buds off, via Rab11, and is recycled back to the plasma membrane by fusing Rab11-positive endosomes with plasma membrane.

Both Rab4 and Rab11 are important in the regulation of human AT$_1$R recycling. Like other small GTPases, Rab4 and

Fig. 11 A model of human AT_1R recycling regulated by Rab4 and Rab11. Rab4 plays a major role in the early stage of AT_1R recycling. During the middle stage, both Rab4 and Rab11 are important in the regulation of AT_1R recycling. Rab11 plays a major role in the late stage of AT_1R recycling. Arrows denote AT_1R transport or fusion between compartments during the recycling period. Due to the space limitation, other important steps such as the initial Rab5 common step[9] and the later step of multiple vesicle bodies[22] are not shown. PM, plasma membrane.

Rab11 have active GTP-bound and inactive GDP-bound forms, which are regulated by their GTPase-activating proteins, guanine nucleotide dissociation inhibitor, and guanine nucleotide exchange proteins.[39,40] The identification of the specific regulators could help us to better understand the regulation of AT_1R recycling.

References

1. P. A. Jose, G. M. Eisner, and R. A. Felder, "The renal dopamine receptors in health and hypertension," *Pharmacol. Ther.* **80**, 149–182 (1998).
2. M. de Gasparo, K. J. Catt, T. Inagami, J. W. Wright, and T. Unger, "International union of pharmacology XXIII. The angiotensin II receptors," *Pharmacol. Rev.* **52**, 415–472 (2000).
3. S. S. G. Ferguson, "Evolving concepts in G protein-coupled receptor endocytosis: the role in receptor desensitization and signaling," *Pharmacol. Rev.* **53**, 1–24 (2001).
4. R. H. Oakley, S. A. Laporte, J. A. Holt, M. G. Caron, and L. S. Barak, "Differential affinities of visual arrestin, β-arrestin 1, and β-arrestin 2 for G protein-coupled receptors delineate two major classes of receptors," *J. Biol. Chem.* **275**, 17201–17210 (2000).
5. Z. Gáborik and L. Hunyady, "Intracellular trafficking of hormone receptors," *Trends Endocrinol. Metab.* **15**, 286–293 (2004).
6. M. Zerial and H. McBride, "Rab proteins as membrane organizers," *Nat. Rev. Mol. Cell Biol.* **2**, 107–117 (2001).
7. J. B. Pereira-Leal and M. C. Seabra, "Evolution of the Rab family of small GTP-binding proteins," *J. Mol. Biol.* **313**, 889–901 (2001).
8. J. L. Seachrist and S. S. Ferguson, "Regulation of G protein-coupled receptor endocytosis and trafficking by Rab GTPases," *Life Sci.* **74**, 225–235 (2003).
9. S. Pfeffer, "Membrane domains in the secretory and endocytic pathways," *Cell* **112**, 507–517 (2003).
10. P. van der Sluijs, M. Hull, A. Zahraoui, B. Goud, and I. Mellman, "The small GTP-binding protein rab4 is associated with early endosomes," *Proc. Natl. Acad. Sci. U.S.A.* **88**, 6313–6317 (1991).
11. S. de Renzis, B. Sonnichsen, and M. Zerial, "Divalent Rab effectors regulate the subcompartmental organization and sorting of early endosomes," *Nat. Cell Biol.* **4**, 124–133 (2002).
12. O. Ullrich, S. Reinsch, S. Urbe, M. Zerial, and R. G. Parton, "Rab11 regulates recycling through the pericentriolar recycling endosome," *J. Cell Biol.* **135**, 913–924 (1996).
13. W. Chen, Y. Feng, D. Chen, and A. Wandinger-Ness, "Rab11 is required for trans-Golgi network-to-plasma membrane transport and a preferential target for GDP dissociation inhibitor," *Mol. Biol. Cell* **9**, 3241–3257 (1998).
14. J. L. Seachrist, P. H. Anborgh, and S. S. G. Ferguson, "β_2-adrenergic receptor internalization, endosomal sorting, and plasma membrane recycling are regulated by rab GTPases," *J. Biol. Chem.* **275**, 27221–27228 (2000).
15. R. H. Moore, E. E. Millman, E. Alpizar-Foster, W. Dai, and B. J. Knoll, "Rab11 regulates the recycling and lysosome targeting of β_2-adrenergic receptors," *J. Cell. Sci.* **117**, 3107–3117 (2004).
16. L. B. Dale, J. L. Seachrist, A. V. Babwah, and S. G. Ferguson, "Regulation of angiotensin II type 1A receptor intracellular retention, degradation, andrecycling by Rab5, Rab7, and Rab11 GTPases," *J. Biol. Chem.* **279**, 13110–13118 (2004).
17. P. H. Anborgh, J. L. Seachrist, L. B. Dale, and S. S. G. Ferguson, "Receptor/β-arrestin complex formation and the differential trafficking and resensitization of β_2-adrenergic and angiotensin II type$_{1A}$ receptors," *Mol. Endocrinol.* **14**, 2040–2053 (2000).
18. G. Innamorati, C. Le Gouill, M. Balamotis, and M. Birnbaumer, "The long and the short cycle. Alternative intracellular routes for trafficking of G-protein-coupled receptors." *J. Biol. Chem.* **276**, 13096–13103 (2001).
19. G. H. Fan, L. A. Lapierre, J. R. Goldenring, and A. Richmond, "Differential regulation of CXCR2 trafficking by Rab GTPases," *Blood* **101**, 2115–2124 (2003).
20. E. Hamelin, C. Thériault, G. Laroche, and J. L. Parent, "The intracellular trafficking of the G protein-coupled receptor TP β depends on a direct interaction with Rab11," *J. Biol. Chem.* **280**, 36195–36205 (2005).
21. L. A. Volpicelli, J. J. Lah, G. Fang, J. R. Goldenring, and A. I. Levey, "Rab11a and myosin Vb regulate recycling of the M4 muscarinic acetylcholine receptor," *J. Neurosci.* **22**, 9776–9784 (2002).
22. L. Hunyady, A. J. Baukal, Z. Gaborik, J. A. Olivares-Reyes, M. Bor, M. Szaszak, R. Lodge, K. J. Catt, and T. Balla, "Differential PI 3-kinase dependence ofearly and late phases of recycling of the internalized AT1 angiotensin receptor," *J. Cell Biol.* **157**, 1211–1222 (2002).
23. Y. Chen, M. Elangovan, and A. Periasamy, "FRET data analysis: the algorithm," in *Molecular Imaging: FRET Microscopy and Spectroscopy*, A. Periasamy and R. N. Day, Eds., pp. 126–145, Oxford University Press, NewYork (2005).
24. A. Periasamy, "Fluorescence resonance energy transfer microscopy: a mini review," *J. Biomed. Opt.* **6**, 287–291 (2001).
25. J. S. Rodman and A. Wandinger-Ness, "Rab GTPases coordinate endocytosis," *J. Cell. Sci.* **113**, 183–192 (2000).
26. P. M. Lanctôt, P. C. Leclerc, E. Escher, R. Leduc, and G. Guillemette, "Role of N-glycosylation in the expression and functional properties of human AT_1 receptor," *Biochemistry* **38**, 8621–8627 (1999).

27. H. Li, I. Armando, P. Yu, C. Escano, S. Mueller, L. Asico, A. Pascua, Q. Lu, X. Wang, V. A. M. Villar, J. E. Jones, Z. Wang, A. Periasamy, Y. S. Lau, P. Soares-da-Silva, K. Creswell, G. Guillemette, D. R. Sibley, G. Eisner, R. A. Felder, and P. A. Jose, "Dopamine 5 receptor mediates Ang II type 1 receptor degradation via a ubiquitin-proteasome pathway in mice and human cells," *J. Clin. Invest.* **118**, 2180–2189 (2008).

28. J. R. Lakowicz, G. Piszczek, and J. S. Kang, "On the possibility of long-wavelength long-life time high-quantum-yield luminophores," *Anal. Biochem.* **288**, 62–75 (2001).

29. G. Apodaca, L. A. Katz, and K. E. Mostov, "Receptor-mediated transcytosis of IgA in MDCK cells is via apical recycling endosomes," *J. Cell Biol.* **125**, 67–86 (1994).

30. Y. Xiang and B. Kobilka, "The PDZ-binding motif of the β_2-adrenoceptor is essential for physiologic signaling and trafficking in cardiac myocytes," *Proc. Natl. Acad. Sci. U.S.A.* **100**, 10776–10781 (2003).

31. M. Tanowitz and M. von Zastrow, "A novel endocytic recycling signal that distinguishes the membrane trafficking of naturally occurring opioid receptors," *J. Biol. Chem.* **278**, 45978–45986 (2003).

32. F. R. Maxfield and T. E. McGraw, "Endocytic recycling," *Nat. Rev. Mol. Cell Biol.* **5**, 121–132 (2004).

33. E. S. Ward, C. Martinez, C. Vaccaro, J. Zhou, Q. Tang, and R. J. Ober, "From sorting endosomes to exocytosis: association of Rab4 and Rab11 GTPases with the Fc receptor, FcRn, during recycling," *Mol. Biol. Cell* **16**, 2028–2038 (2005).

34. D. Sheff, L. Pelletier, C. B. O'Connell, G. Warren, and I. Mellman, "Transferrin receptor recycling in the absence of perinuclear recycling endosomes," *J. Cell Biol.* **156**, 797–804 (2002).

35. J. Gruenberg, "The endocytic pathway: a mosaic of domains," *Nat. Rev. Mol. Cell Biol.* **2**, 721–730 (2001).

36. J. L. Rosenfeld, B. J. Knoll, and R. H. Moore, "Regulation of G-protein-coupled receptor activity by rab GTPases," *Recept. Channels* **8**, 87–97 (2002).

37. D. Roosterman, O. J. Kreuzer, N. Brune, G. S. Cottrell, N. W. Bunnett, W. Meyerhof, and M. Steinhoff, "Agonist-induced endocytosis of rat somatostatin receptor 1," *Endocrinology* **148**, 1050–1058 (2007).

38. D. F. Guo, I. Chenier, V. Tardif, S. N. Orlov, and T. Inagami, "Type 1 angiotensin II receptor-associated protein ARAP1 binds and recycles the receptor to the plasma membrane," *Biochem. Biophys. Res. Commun.* **310**, 1254–1265 (2003).

39. M. C. Seabra and C. Wasmeier, "Controlling the location and activation of Rab GTPases," *Curr. Opin. Cell Biol.* **16**, 451–457 (2004).

40. R. S. Goody, A. Rak, and K. Alexandrov, "The structural and mechanistic basis for recycling of Rab proteins between membrane compartments," *Cell. Mol. Life Sci.* **62**, 1657–1670 (2005).